

2 General Relativity and Black Holes

- Black holes are a prediction of Einstein's **Theory of General Relativity**, and as such date from circa 1916. They are defined as a compact star from which nothing, not even light cannot escape, due to the pull of gravity.
- As such, the concept of a black hole pre-dates Einstein, and was originally proposed in the context of Newtonian gravity by George Mitchell in 1783.

C& O
Sec. 17.1

2.1 Gravitational Time Dilation and Light Bending

- From this principle the phenomenon of the **gravitational redshift of light** can quickly be deduced. Consider a photon emitted at the top of an elevator of height h . If the elevator is accelerated upwards at g , then it will have moved a distance $s = gt^2/2$ when the photon strikes the elevator floor in a time $t \approx h/c$. The speed of the elevator will then be $v = gt \approx gh/c$.

C & O,
pp. 617-22

Plot: Equivalence Principle for Vertically Traveling Light

The Doppler shift (in this case a blueshift) of the light would then satisfy

$$\frac{\Delta\nu}{\nu} = \frac{v}{c} = \frac{gh}{c^2} = \frac{\Delta\phi}{c^2} \quad , \quad (12)$$

where $\Delta\phi = gh$ is the equivalent gravitational potential the photon traverses in its elevator journey. From the Equivalence Principle, one infers that a light will change its frequency according to $\Delta\nu/\nu = -gh/c^2$ when emerging from a deep gravitational potential gh , i.e. *light is redshifted by gravity*. Thus, for photons, the quanta of light, *gravity does work on their energy*.

- An equivalent statement of this phenomenon is that a gravitational field induces **time dilation** according to an observer at infinity, described by $\Delta t/t = \Delta\phi/c^2$. In other words, *clocks tick slower in a gravitational field*.

Gravitational Time Dilation

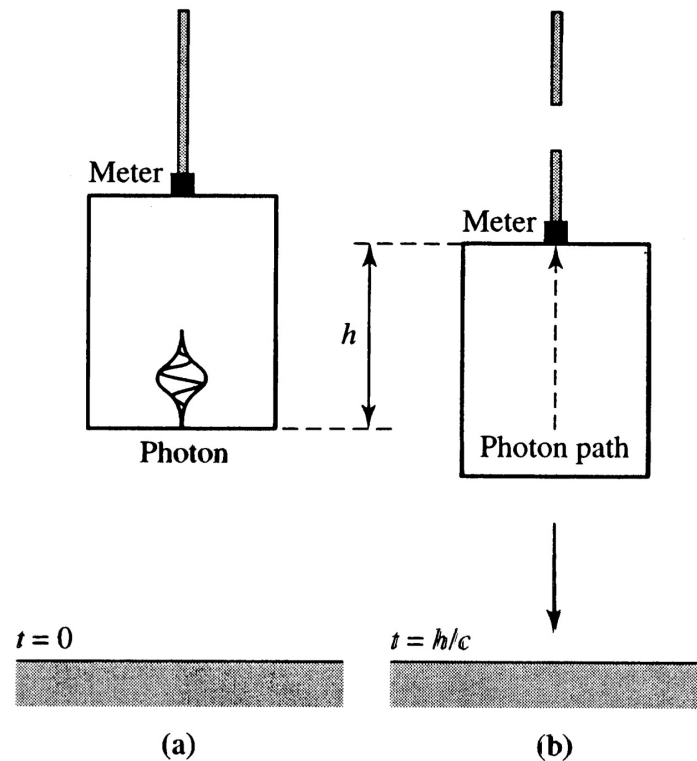


FIGURE 17.11 Equivalence principle for a vertically traveling light. The photon (a) leaves the floor at $t = 0$, and (b) arrives at the ceiling at $t = h/c$.

- Elevator equivalence principle *gedanken* experiment for **time dilation** and **gravitational redshift**. From [Carroll & Ostlie, *An Introduction to Modern Astrophysics*](#).

- A beautiful illustration of time dilation is manifested in **Shapiro delay**, which is the net time delay measured from a star that is eclipsed by another. This was done for the case of the edge-on binary pulsar J0737-3039A/B, where pulsation delay can be cleanly measured.

- * The J0737-3039A/B case not only vindicates gravitational time dilation, but enables measurement of a number of orbital general relativistic parameters and the respective stellar masses to impressive precision.

Plot: Shapiro Delay Signal from PSR J0737-3039A/B

- Now consider a photon traversing the same accelerating elevator, but this time from side to side. By a similar analysis, the time of flight across the elevator is w/c and the elevator will have moved a vertical distance $s = gt^2/2 \approx g(w/c)^2/2$ when the photon hits the far side of the wall. The photon is then perceived to have followed a curved path with an angular deflection

$$\Delta\theta \approx \frac{s}{w} \approx \frac{gw}{2c^2} \tag{13}$$

from a horizontal trajectory.

Plot: Equivalence Principle for Horizontally Traveling Light

The Equivalence Principle then indicates **gravitational light bending**. Using $g = GM/r^2$ for the field at a distance r from mass M , we have

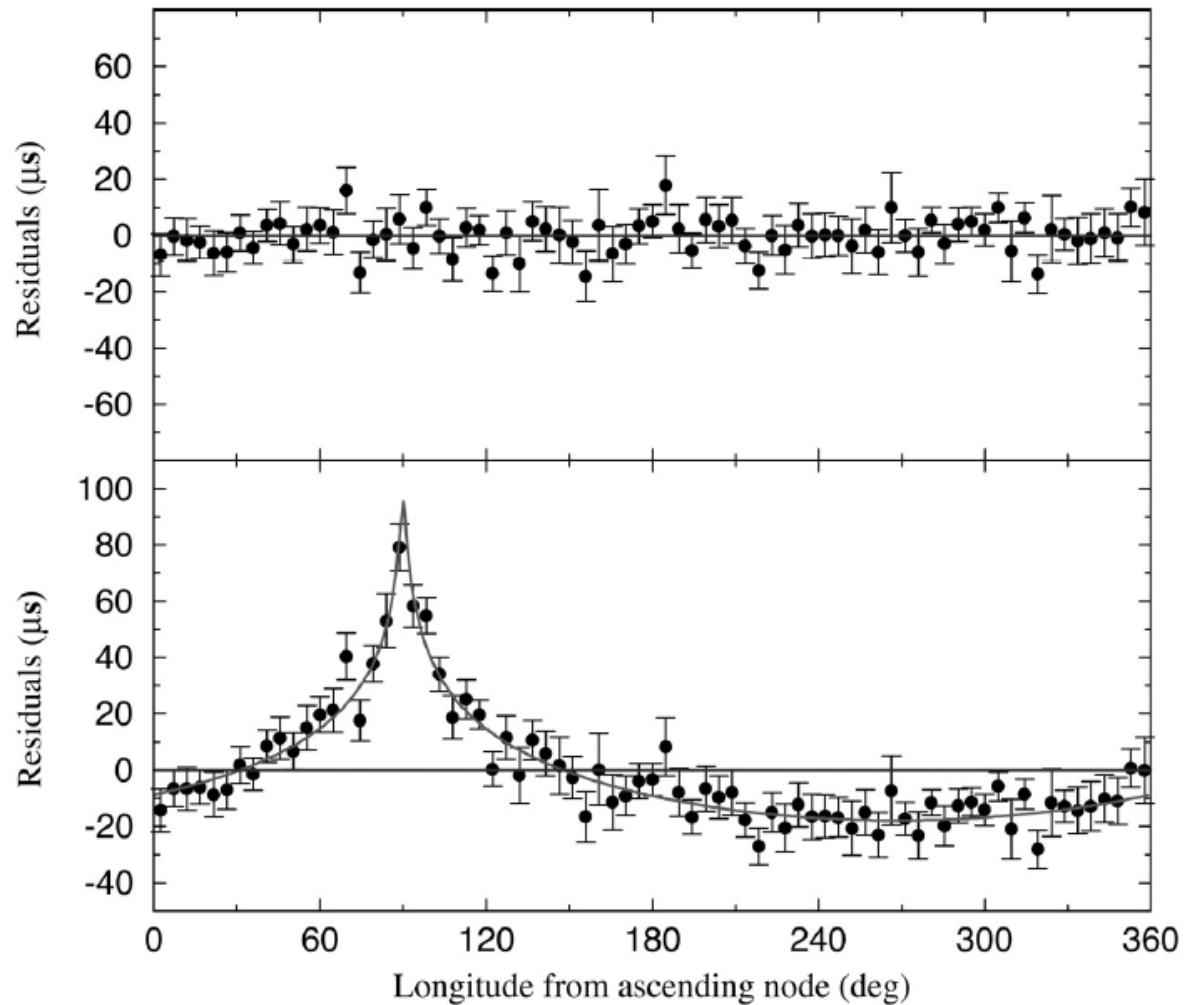
$$\Delta\theta \sim \frac{GM}{rc^2} \equiv \frac{R_s}{2r} \tag{14}$$

as the bending of light, setting $w \rightarrow 2r$. Here $R_s = 2GM/c^2$ is the gravitational radius, widely known as the **Schwarzschild radius**. This marks the departure of spacetime from a Euclidean/Minkowskian genre.

Plot: Light bending Geometry

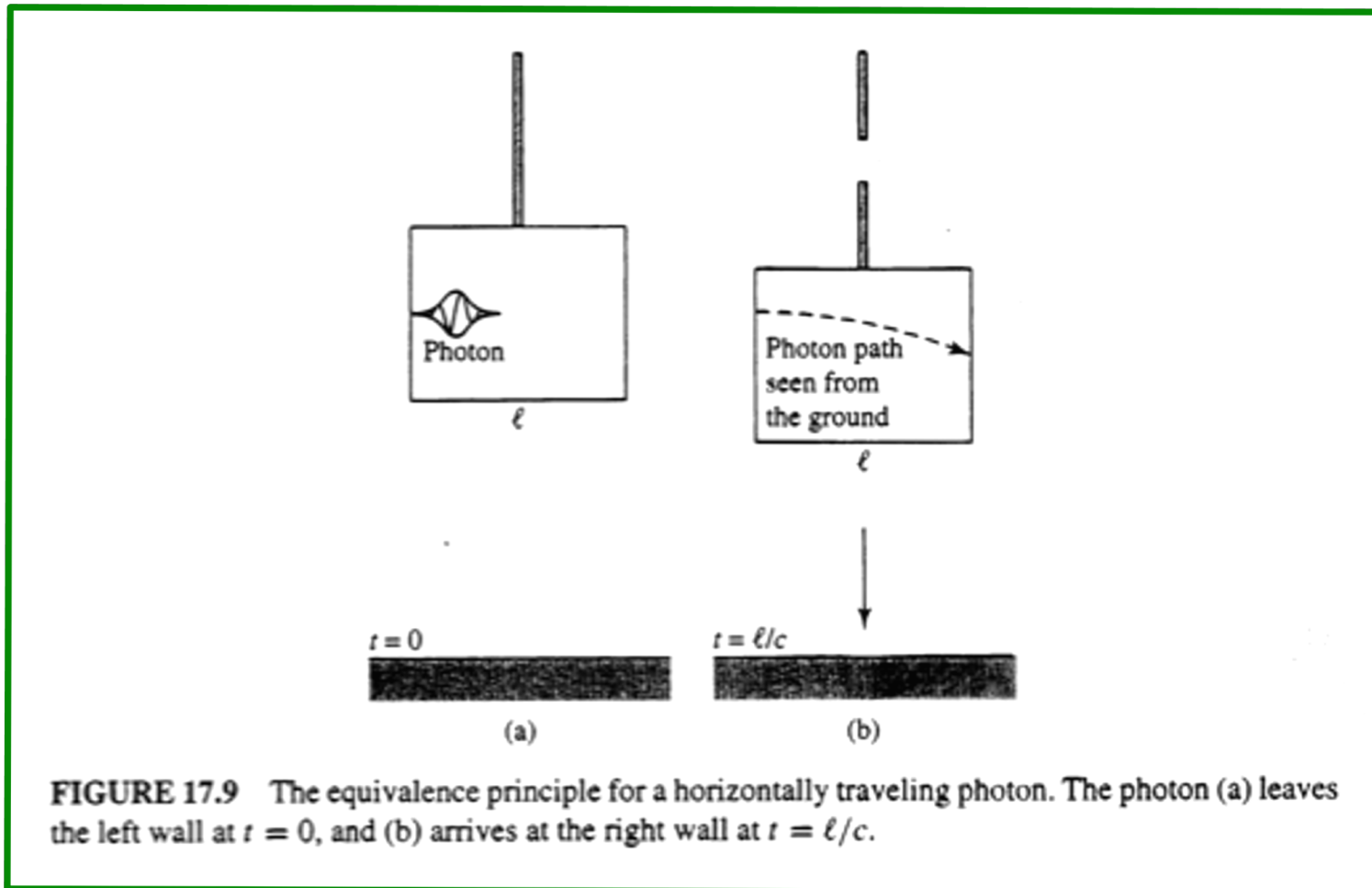
Binary Pulsar J0737-3039A/B

General Relativistic Shapiro Delay



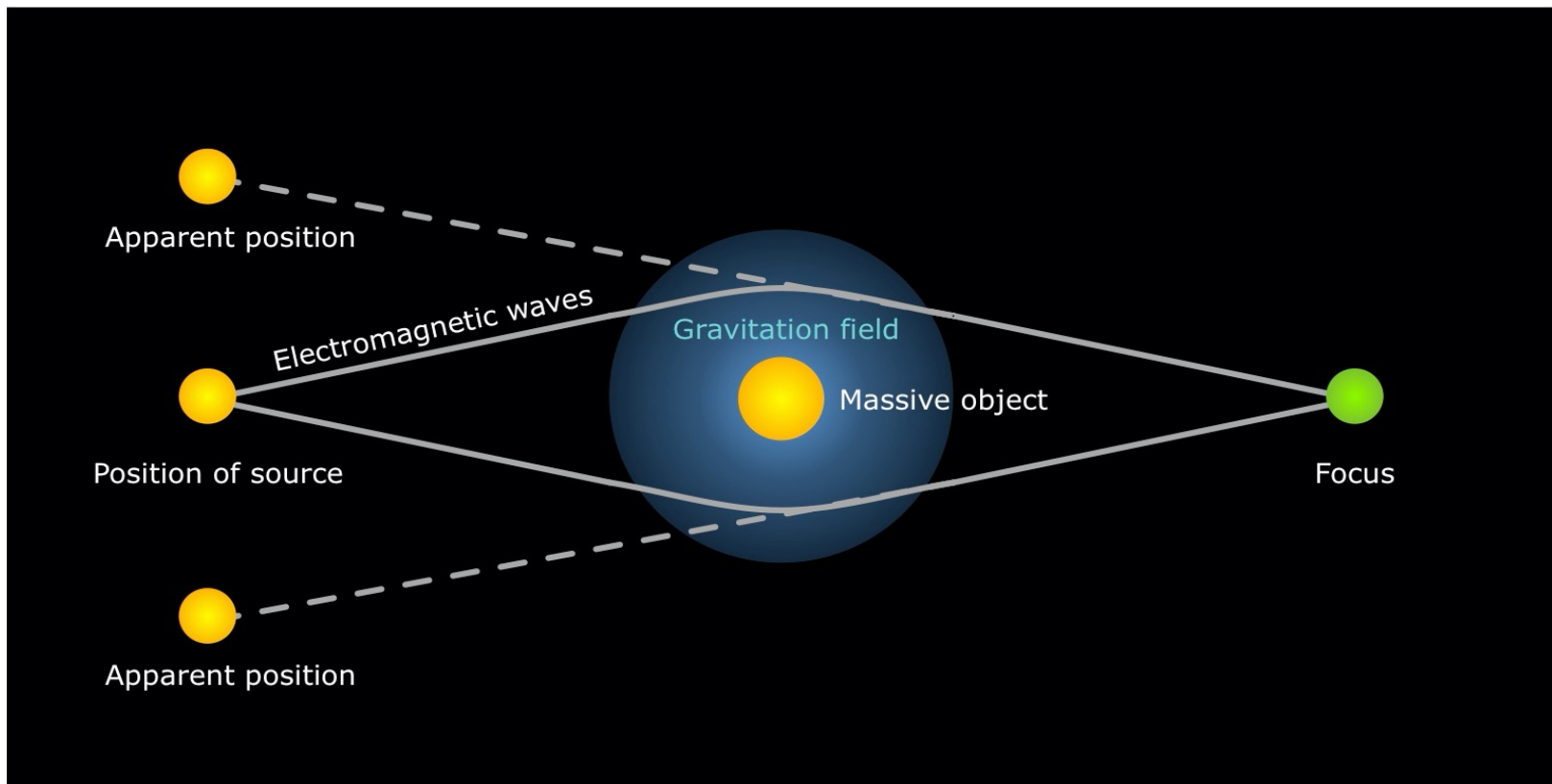
Lyne et al.
(Science 2004)

Gravitational Light Bending



- Elevator equivalence principle *gedanken* experiment for **gravitational light bending**. From [Carroll & Ostlie, *An Introduction to Modern Astrophysics*](#).

Gravitational Light Bending Geometry



- The bending of light was a core prediction of Einstein’s theory of General Relativity (GR). The principle test was to measure deflections of starlight in occultations by the sun. The only way to do this was during a solar eclipse by the moon, so it was first done in 1919. GR theory was vindicated nicely.

Plot: Light Deflection Tests of General Relativity

2.2 Precession of the Perihelion of Mercury

Since light trajectories are curved in the neighborhood of massive stars, and the Equivalence Principle states that it should travel at the same speed c and in a straight line in the local inertial (free falling) frame, then spacetime must be distorted near masses. In terms of stellar or planetary orbital dynamics, GR introduces departures from the inverse square force law of Newton:

$$V(r) = -\frac{GM}{r} \left\{ 1 + \epsilon(\vec{r}, t) \right\} . \quad (15)$$

This automatically implies that ellipses are no longer exact solutions to the orbital motion. The cumulative influence, when $\epsilon = O(R_s/r)$ is small, is an epicyclic motion with a gradual precession of the orbital periastron.

- This provided a second observational test of Einstein’s theory, via the **precession of the perihelion of Mercury**. The evolving pseudo-ellipse is

$$r = \frac{a(1 - e^2)}{1 + e \cos(\phi - \phi_p)} , \quad \phi_p = \phi_p(t) \approx \Delta\phi_p \frac{t}{P} . \quad (16)$$

The gravitational modification to the orbital dynamics is then

$$\Delta\phi_p = \frac{6\pi}{1 - e^2} \frac{GM_\odot}{ac^2} \quad (17)$$

per orbit. For Mercury, this prediction is 43 seconds of arc per century, a small correction to Newtonian orbits.

- To test one must allow for a Newtonian tidal term in the orbital dynamics due to the **oblateness of the sun**, that is 532”/century. Einstein was again proven correct, for Mercury, Venus and Earth!

Plot: Precession of Planetary Perihelia

Stellar Light Deflection near Solar Limb

- Table 8.1 of *Weinberg Gravitation and Cosmology*

Eclipse	Site	Number of Stars	r_0/R_\odot	θ_\odot (sec)	Ref.
May 29, 1919	Sobral	7	2-6	1.98 ± 0.16	a
	Principe	5	2-6	1.61 ± 0.40	a
September 21, 1922	Australia	11-14	2-10	1.77 ± 0.40	b
	Australia	18	2-10	1.42 to 2.16	c
	Australia	62-85	2.1-14.5	1.72 ± 0.15	d
	Australia	145	2.1-42	1.82 ± 0.20	e
May 9, 1929	Sumatra	17-18	1.5-7.5	2.24 ± 0.10	f
June 19, 1936	U.S.S.R.	16-29	2-7.2	2.73 ± 0.31	g
	Japan	8	4-7	1.28 to 2.13	h
May 20, 1947	Brazil	51	3.3-10.2	2.01 ± 0.27	i
February 25, 1952	Sudan	9-11	2.1-8.6	1.70 ± 0.10	j

c.f. 1.75''

^a F. W. Dyson, A. S. Eddington, and C. Davidson, *Phil. Trans. Roy. Soc.*, **220A**, 291 (1920); *Mem. Roy. Astron. Soc.*, **62**, 291 (1920).
^b G. F. Dodwell and C. R. Davidson, *Mon. Nat. Roy. Astron. Soc.*, **84**, 150 (1924).
^c C. A. Chant and R. K. Young, *Publ. Dominion Astron. Obs.*, **2**, 275 (1924).
^d W. W. Campbell and R. Trumpler, *Lick Observ. Bull.*, **11**, 41 (1923); *Publ. Astron. Soc. Pacific*, **35**, 158 (1923).
^e W. W. Campbell and R. Trumpler, *Lick Observ. Bull.*, **13**, 130 (1928).
^f E. F. Freundlich, H. v. Klüber, and A. v. Brunn, *Ab. Preuss. Akad. Wiss.*, No. 1, 1931; *Z. Astrophys.*, **3**, 171 (1931).
^g A. A. Mikhailov, *C. R. Acad. Sci. USSR (N. S.)*, **29**, 189 (1940).
^h T. Matukuma, A. Onuki, S. Yosida, and Y. Iwana, *Jap. J. Astron. and Geophys.*, **18**, 51 (1940).
ⁱ G. van Biesbroeck, *Astron. J.*, **55**, 49, 247 (1949).
^j G. van Biesbroeck, *Astron. J.*, **58**, 87 (1953).

Precession of Planetary Perihelia

Table 8.3. Comparison of Theoretical and Observed Centennial Precessions of Planetary Orbits.⁶

Planet	a (10^6 km)	e	$\frac{6\pi MG}{L}$	Revolutions Century	$\Delta\varphi$ (seconds/century)	
					Gen. Rel.	Observed
Mercury (♃)	57.91	0.2056	0.1038"	415	43.03	43.11 \pm 0.45
Venus (♀)	108.21	0.0068	0.058"	149	8.6	8.4 \pm 4.8
Earth (♁)	149.60	0.0167	0.038"	100	3.8	5.0 \pm 1.2
Icarus	161.0	0.827	0.115"	89	10.3	9.8 \pm 0.8

- Rates of **precession of the perihelia** of **Mercury, Venus, Earth and Icarus**,* after subtraction of multi-body contributions within the solar system to Newtonian orbital dynamics. Here $L=a(1-e^2)$. From **Weinberg *Gravitation and Cosmology***.
 - * **Icarus** is an **Apollo asteroid** (one with a perihelion < 1 AU) with a period of 1.12 years.
- The measured precession confirmed **Einstein's theory** to very good precision.

2.3 Einstein's Field Equations: Schwarzschild Metric

The complete mathematical theory that describes general relativity is encapsulated in Einstein's **field equations**:

C & O,
Sec. 17.2

$$G^{\mu\nu} = \frac{8\pi G}{c^4} T^{\mu\nu} \quad . \quad (18)$$

Here $G^{\mu\nu}$ describes spacetime distortion via the second order derivative of the metric tensor $g^{\mu\nu}$, and $T^{\mu\nu}$ represents the energy/momentum stress tensor (matter + light + E/M fields). This is a matrix system of 16 partial differential equations.

- Mass/gravity therefore distorts spacetime, and produces curved **geodesics** i.e. non-rectilinear light paths.
- Apart from gravitational redshift/time dilation already mentioned, mass increases the volume in a local inertial frame and generates angular distortion. Both are germane to cosmology.
- Shortly after the publication of Einstein's theory, Karl Schwarzschild derived (1916) the solution of the field equations in the case of a spherically-symmetric potential (isotropy) that is time-independent. In spherical polar coordinates for an observer at infinity, the **Schwarzschild metric** is

$$c^2 d\tau^2 = g^{\mu\nu} dx_\mu dx_\nu \equiv B(r) c^2 dt^2 - \frac{dr^2}{B(r)} - r^2 (d\theta^2 + \sin^2 \theta d\phi^2) \quad (19)$$

where the last two terms are the angular portion, and

$$B(r) = 1 - \frac{2GM}{rc^2} \equiv 1 - \frac{R_s}{r} \quad , \quad R_s = \frac{2GM}{c^2} \quad . \quad (20)$$

Here R_s is the **Schwarzschild radius** that defines a coordinate singularity as identified by an observer at infinity. The **proper time** τ is the clock according to an inertial or free-falling observer approaching the mass.

* For finite dt , we have $d\tau \rightarrow \infty$ as $r \rightarrow R_s$, which is also known as the **event horizon**. This means that we at infinity perceive that an object falling into a black hole never actually gets there, but for the object, it takes a finite amount of time to cross the event horizon.

2.4 Black Holes

- An object whose entire physical extent is interior to its Schwarzschild radius is defined to be a **black hole**.

C & O,
Sec. 17.3

- The key marker of the physical conditions governing a black hole is that the escape speed v_{esc} of a particle is comparable to the speed of light:

$$\frac{v_{esc}}{c} \sim \sqrt{\frac{GM}{r c^2}} \sim 1 \quad \Rightarrow \quad r \sim \frac{GM}{c^2} \quad . \quad (21)$$

This result [*obtainable purely from dimensional analysis*] is independent of particle mass and approximately defines the **Schwarzschild radius**.

- The presence of a black hole is normally inferred from its pull and/or interaction with its environs (e.g. the Galactic Centre)

Plot: Mass determinations at the Galactic Centre

* Dynamical data are particularly useful for identifying candidate black holes in the Milky Way. The principal technique is using Kepler's Third Law and line spectroscopy to determine radial (line-of-sight) velocities v_{1r} of the BH companion. This gives a **mass function** (for circular, $e = 0$, orbits):

$$f(m_1) = \frac{m_1^3}{(m_2 + m_1)^2} \sin^3 i = \frac{P}{2\pi G} v_{2r}^3 \quad . \quad (22)$$

for an orbit inclined at angle i to the plane of the sky.

Plot: Table of Galactic Black Hole Candidates

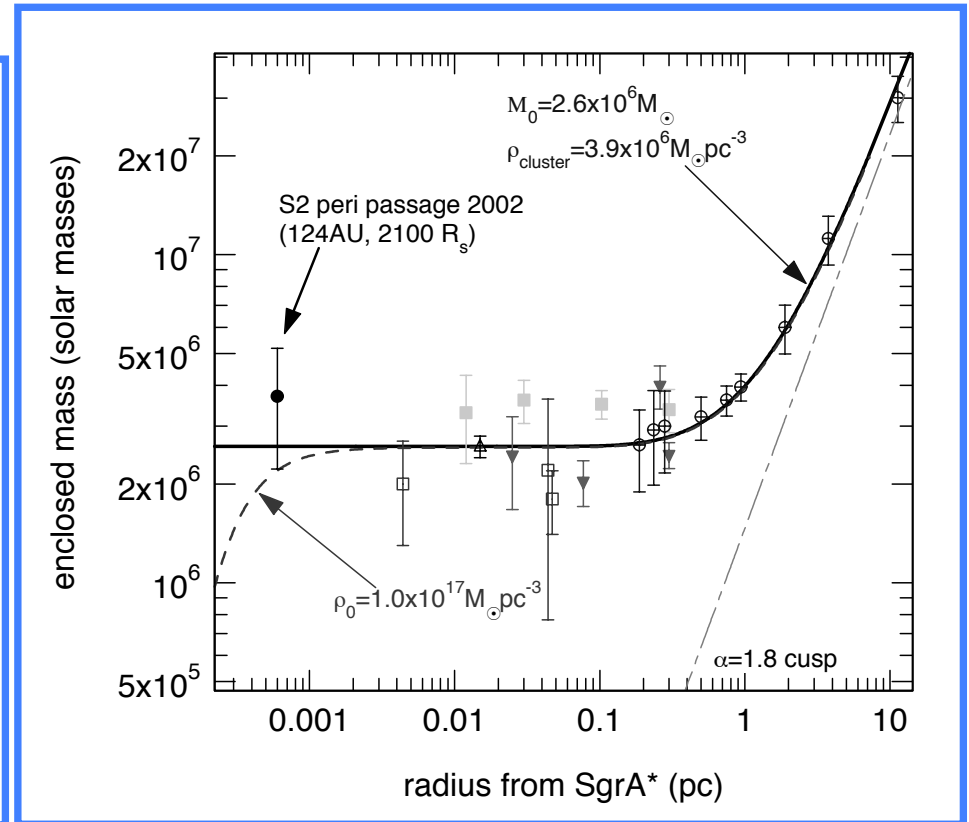
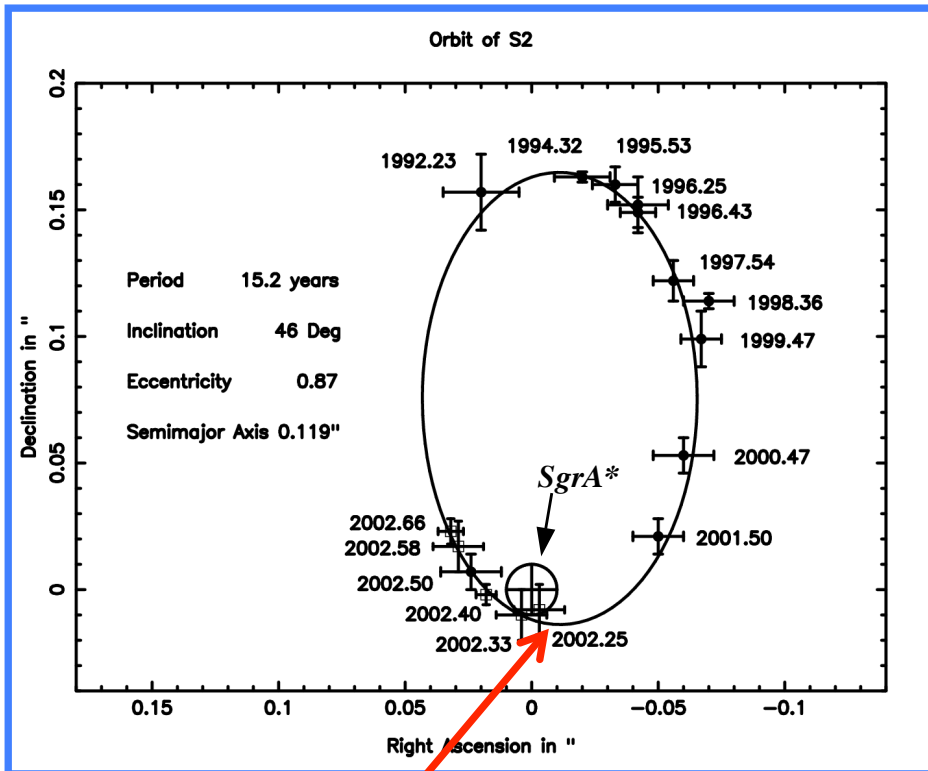
- Key astrophysical signatures of black holes are (i) observational: X-ray and γ -ray emission, rapid variability; (ii) physical: accretion disks, and jets.

* efficient energy conversion via tapping of $E = mc^2$.

- The best imaging observation to date of a black hole's environs is the central SMBH of M87 by the **Event Horizon Telescope** (EHT).

Stellar Passages Near the Galactic Centre

Schoedel et al. (2002, Nature 419, 694)



- **Left Panel:** passage of the star S2 in the epoch 1992-2002, which has a Keplerian period of 15 years, imaged in IR using ESO's VLT in Chile, capturing **peribothron** (pericentre) portion cleanly.
- Pericentre offset of 17.2 light hours (124 AU) rules out the presence of **fermion balls** and promotes the existence of a central supermassive black hole (SMBH) of mass $3.7 \times 10^6 M_\odot$.
- **Right Panel:** enclosed mass distribution and the S2 data point favoring a SMBH for Sgr A*.

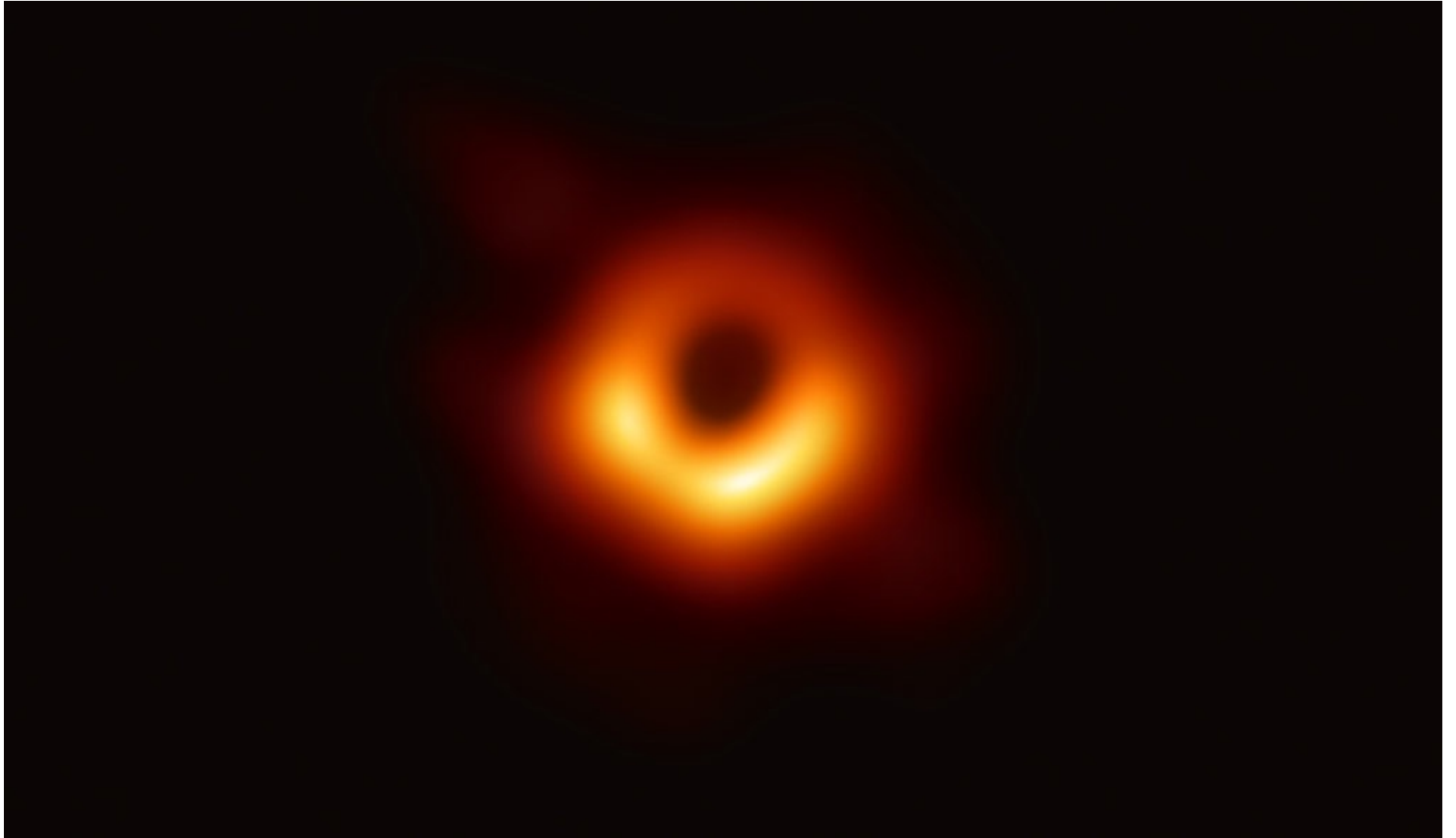
Black Hole Masses in Binaries

Table 4.2. *Confirmed black hole binaries: X-ray and optical data*

Source	f(M) ^a (M _⊙)	M ₁ ^a (M _⊙)	f(HFQPO) (Hz)	f(LFQPO) (Hz)	Radio ^b	E _{max} ^c (MeV)	References
0422+32	1.19±0.02	3.2–13.2	–	0.035–32	P	0.8,1–2:	1,2,3,4,5
0538–641	2.3±0.3	5.9–9.2	–	0.46	–	0.05	6,7
0540–697	0.14±0.05	4.0–10.0:	–	0.075	–	0.02	8,7
0620–003	2.72±0.06	3.3–12.9	–	–	P,J?	0.03:	9,10,11,11a
1009–45	3.17±0.12	6.3–8.0	–	0.04–0.3	– ^d	0.40, 1:	12,4,13
1118+480	6.1±0.3	6.5–7.2	–	0.07–0.15	P	0.15	14,15,16,17
1124–684	3.01±0.15	6.5–8.2	–	3.0–8.4	P	0.50	18,19,20,21
1543–475	0.25±0.01	7.4–11.4 ^e	–	7	– ^f	0.20	22,4
1550–564	6.86±0.71	8.4–10.8	92,184,276	0.1–10	P,J	0.20	23,24,25,26,27
1655–40	2.73±0.09	6.0–6.6	300,450	0.1–28	P,J	0.80	28,29,30,31,54
1659–487	> 2.0 ^g	–	–	0.09–7.4	P	0.45, 1:	32,33,4,13
1705–250	4.86±0.13	5.6–8.3	–	–	– ^d	0.1	34,35
1819.3–2525	3.13±0.13	6.8–7.4	–	–	P,J	0.02	36,37
1859+226	7.4±1.1	7.6–12:	190	0.5–10	P,J?	0.2	38,39,40,41
1915+105	9.5±3.0	10.0–18.0:	41,67,113,168	0.001–10	P,J	0.5, 1:	42,43,44,4,13
1956+350	0.244±0.005	6.9–13.2	–	0.035–12	P,J	2–5	45,46,47,48,49
2000+251	5.01±0.12	7.1–7.8	–	2.4–2.6	P	0.3	18,50,51
2023+338	6.08±0.06	10.1–13.4	–	–	P	0.4	52,53

- Dynamical estimates of Galactic black hole masses (highlighted M_1 column) – cases confirmed by radio and optical observations of the orbiting companion.
- From [McClintock and Remillard \(2004\)](#) in "Compact Stellar X-ray Sources," eds. W.H.G. Lewin & M. van der Klis, Cambridge University Press. [[astro-ph/0306213](#)]

M87 SMBH Image Event Horizon Telescope (EHT)



Credit: EHT Collaboration